Research Square

Preprints are preliminary reports that have not undergone peer review.
They should not be considered conclusive, used to inform clinical practice,
or referenced by the media as validated information.

Direct conversion of industrial off gas to green carbonate and H2

Mingyue Ding

dingmy@whu.edu.cn

Wuhan University https://orcid.org/0000-0001-8769-4153

Hou GuoQiang

Wuhan University

Jinzhe Zhang

Wuhan University

Di Xu

Wuhan University

Jinjin Peng

Wuhan University

Yangyang Li

Wuhan University

RuoSong He

Wuhan University

Siyi Huang

Wuhan University

HanZhu Zhang

Wuhan University

Xiaochuan Wang

Wuhan University

Xiang-Kui Gu

Wuhan University https://orcid.org/0000-0001-6537-7026

Article

Keywords:

Posted Date: November 23rd, 2026

DOI: https://doi.org/10.21203/rs.3.rs-11400211/v1

License: This work is licensed under a Creative Commons Attribution 4.0 International License.
Read Full License

Additional Declarations: There is **NO** Competing Interest.

Direct conversion of industrial off gas to green carbonate and H_2

Guoqiang Hou[a#], Jinzhe Zhang[a#], Jinjin Peng[a], SiYi Huang[a], YangYang Li[a], RuoSun He[a], HanZhu Zhang[a], Xiaochuan Wang[c], Xiang-Kui Gu[a], Di Xu[a*], Mingyue Ding[a,b]**

[a] School of Power and Mechanical Engineering, Wuhan University; Wuhan 430072, China.

b Perception and Effectiveness Assessment for Carbon-neutrality Efforts, Engineering Research Center of Ministry of Education, Institute for Carbon Neutrality, Wuhan University; Wuhan 430072, China.

c The Institute of Technological Sciences, Wuhan University; Wuhan 430072, China.

E-mail: x_d@whu.edu.cn, xiangkuigu@whu.edu.cn, dingmy@whu.edu.cn

Abstract:

Decarbonization of steel and coal-chemical industries, a major CO_2 emitter, is crucial for achieving carbon neutrality. Escaping the grip of combustion, separation and hydrogenation, is a formidable challenge on the path to industry net-zero carbon emissions. Here we suggest a non-hydrogenated new route for directly converting industrial off-gas and methanol into green dimethyl carbonate (DMC) and clean H_2 via coupling off-gas conversion and methanol upgrading. In the design, the CO in off-gas reacts with the byproduct H_2O generated during CO_2-to-DMC synthesis, continuously pulling DMC synthesis equilibrium forward following Le Chatelier's principle, while yielding H_2 as a valuable co-product. This process exhibits significant advantages in carbon retention, cost-effectiveness and H_2 production, and covers various compositions of steelmaking and gasification off-gases. Notably, a DMC yield of 76.8 mmol/g with >98% selectivity is obtained on the new route, which represents 7.8-fold higher than conventional sole CO_2 route, together with 74.6 mL/g H_2. The strategy converts the industrial off-gases utilization from a costly separation and high H_2 demand challenge into a reaction advantage for simultaneous DMC synthesis and H_2 production, providing a new approach for industrial decarbonization and MeOH upgrading.

Main text

The iron/steel and coal-chemical industries are major contributors to greenhouse-gas emissions, together emitting more than 3 Gt of CO_2 per year(*1, 2*). The carbon of these emissions mainly originates from co-produced CO and CO_2 from ironmaking, coal gasification and downstream synthesis(*3, 4*). With demand of the heavy industrial products growing, decarbonizing of the high-emission industries are imperative(*5*). Currently, the carbon-rich streams are usually used as internal fuels for heat and power via combustion, whereby CO is converted into additional CO_2, exacerbating further emissions and foregoes chemical value of CO for more sustainable options(*3, 6*) (Fig. 1a). In conversion path, catalytic hydrogenation to fuels and chemicals is being developed to recover the carbon value of industrial off-gases (*7, 8*)(Fig. 1a). However, hydrogenation-based carbon reduction route shows a pronounced trade-off between carbon retention, H_2 demand and cost. For example, fuel and light-olefin synthesis retain only 44.9%-58.3% of the feed carbon on a CO_2-equivalent feed basis, with an extremely high H_2 consumption of 137 kg/t (Fig. 1b and Table S1-S11)(*9*). Methanol and methane synthesis can raise carbon retention up to 90%, yet they require H_2 inputs of 123.7 and 164.9 kg/t, respectively, and

incur high net costs reaching US$885/t (Fig. 1b and Table S11)(*9*). The RWGS reaction reduces H_2 demand to 45.8 kg/t, but it generates CO. Further upgrading of CO requires additional H_2, so high H_2 consumption remains a persistent challenge. Noted that the above process is based on the separation and purification of CO and CO_2 in the off-gas. As is well known, this is a highly energy-consuming process. The development of non-hydrogenated, more efficient and cost-effective route for the direct conversion of carbon-rich off-gas is a key scientific issue to be resolved in this area.

Methanol (MeOH), a key C1 platform compound, can be upgraded into multi-carbon products, offering a practical and promising route for sustainable chemical manufacturing. The co-conversion of off-gas and MeOH to green dimethyl carbonate provides a sustainable route for linking off-gas non-hydrogenated utilization with MeOH upgrading (*1, 10-12*). However, the reaction of CO_2 with CH_3OH to DMC and H_2O is severely restricted by thermodynamic equilibrium ($\triangle_r G_m^\theta$ = +26.21 kJ/mol), resulting in intrinsically low product yields (<1%) and very poor CO_2 utilization efficiency (Table S12-14), and it is believed that ought to be more challenging than the kinetics factors for its applications. Moreover, the inevitable formation of H_2O byproduct drives the equilibrium toward reactants, further inhibiting DMC formation (*13-17*). According to Le Chatelier's principle, decreasing the activity of a product can shift an equilibrium toward product formation; in DMC synthesis system, lowering the activity of H_2O by one order of magnitude provides 7.9 kJ mol^{-1} of thermodynamic driving force, significantly breaking the thermodynamic equilibrium limitation (Table S15). Therefore, rational design of the reaction network to achieve cost-effective in-situ consumption of byproduct H_2O and overcome thermodynamic equilibrium constraints represents the core strategy to break the major bottleneck and enhance carbon conversion efficiency.

Here, by coupling industrial off-gas conversion and methanol upgrading, we propose a new industrial off-gas utilization route that directly converts CO and CO_2 in off-gas with methanol into DMC with co-production of H_2. In this design, CO is supposed to in-situ convert the by-product H_2O of CO_2-to-DMC synthesis via low-temperature water-gas shift reaction (LT-WGS), and simultaneously drive the DMC-forming equilibrium forward while producing clean H_2 as a valuable co-product. The overall transformation can be written as (1-x) CO_2 + xCO + $2CH_3OH \rightarrow CH_3OCOOCH_3$ + xH_2+ (1-x) H_2O. At CO_2 equivalent feed, the new route could retain 87.0% of the feed carbon in DMC, exceeding the carbon retention of fuels and light olefins (Table S11). Crucially, it requires no external H_2 and instead co-produces 15.9 kg H_2/t. After accounting for DMC and H_2 product credits, its net cost is only US$169 t^{-1}, 70-81% lower than those of the H_2 intensive fuel and chemical routes (Table S11). Importantly, the designed reaction exhibits significantly favorable thermodynamics compared with traditional CO_2-to-DMC route (Table S17-20). The standard Gibbs free energy is -4.71 kJ/mol, much lower than +26.21 kJ/mol of traditional CO_2 route (Fig. 1c). Correspondingly, the equilibrium conversion can reach to 25.4% on the off-gas conversion route, an 18-fold enhancement the conventional CO_2 route (Fig. 1d). On a simple proof-of-concept catalyst, the new route gives a 76.8 mmol/g of DMC yield with near 100% selectivity, together with the co-production of 74.6 mL/g H_2. The DMC yield is 3~7 times that achieved

by the reported traditional system (Fig. 1e, Table S21). This off-gas and methanol co-conversion system open up new non-redox strategies for the high-value utilization of off-gas and MeOH upgrading synergistically in a thermodynamically favorable route.

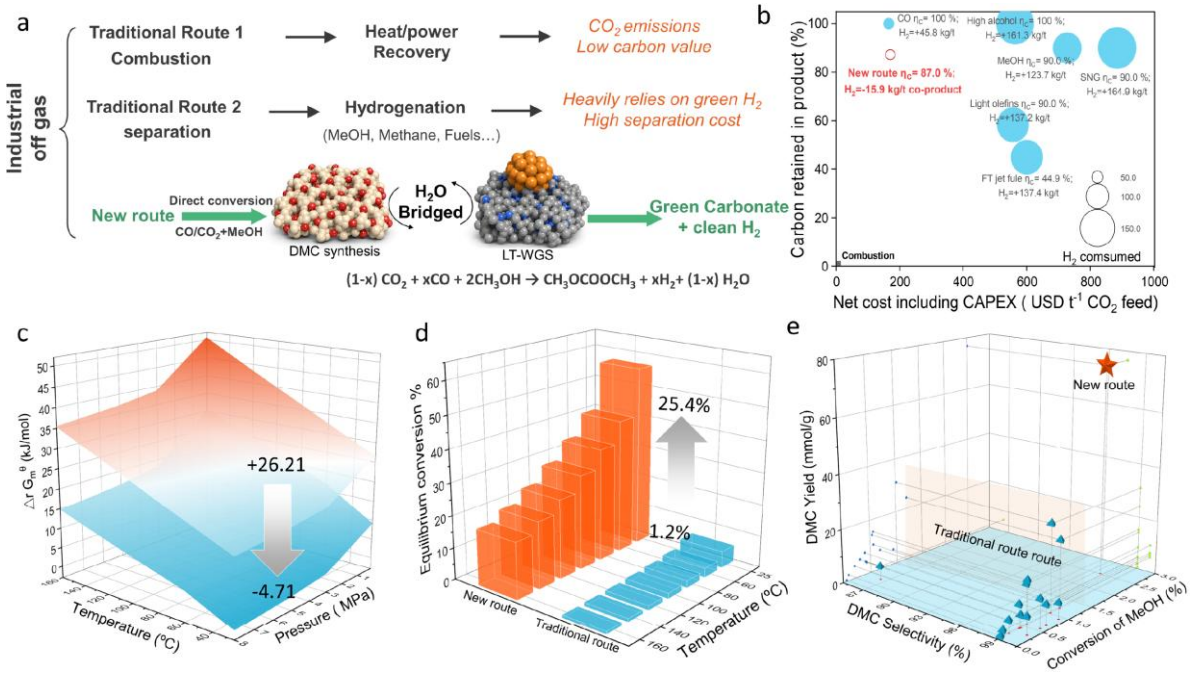


Fig. 1. Design of the coupling of off-gas conversion and MeOH upgrading. (a) Conventional off-gas utilization routes and the proposed route for DMC and H_2 co-production. (b) Comparison of carbon retention, H_2 demand, and net cost among off-gas utilization routes. (c) Gibbs free energy, (d) Equilibrium conversion of conventional CO_2 to DMC synthesis and off-gas and MeOH conversion to DMC and H_2. (e) Comparison of DMC yield, selectivity for the off-gas to DMC and reported CO_2 to DMC.

Direct conversion of off-gas to DMC and H_2

To achieve the coupling of DMC synthesis and LT-WGS, defective CeO_2-600 and Au/MoC-α are selected as catalyst example for indicating the concept in this work, respectively(*18, 19*). A series of characterizations confirm that CeO_2-600 exhibits defect-rich fluorite nanorods structure (Fig. S1-S4). Localized distortion of Ce–O bonds within nanorods create electron-enriched lattice oxygen sites, which facilitate CO_2 activation and weakened MeOH adsorption, correspondingly enhancing $*CH_3O$-$*CO_2$ coupling to produce DMC (Fig. S5-S9). In parallel, 2%AuMoC-α comprises porous MoC-α nanocrystals supported with atomically dispersed Au species and 1-2 nm Au clusters (Fig. S10-S12). Strong Au-MoC interaction results in an electron-enriched Au-MoC interface, enabling CO adsorption and H_2O dissociation simultaneously (*20, 21*) (Fig. S13-16). These structural features provide the basis for the complementary DMC synthesis and LT-WGS functions of the two catalysts (Fig. S17-18).

The two catalysts were then fully stirred at 800 rpm in the reactor for 30 minutes to achieve direct conversion of off-gas with MeOH to DMC and H_2. The mixed proof-of-concept catalyst shows a disordered distribution with nanoscale intimacy (Fig. S19-20). When tested with a CO/CO_2 mixture of 3:2 simulating CO-rich industrial off-gas, the system obtains a much higher DMC yield of 66.9 mmol/g with nearly 100% selectivity and 63.7 mL/g of clean H_2 co-production (Fig. 2a-b). Then, the mixed catalyst was evaluated using CO/CO_2 mixtures representative of major industrial off-gases. These

streams span a broad compositional window, from CO_2-rich COREX/FINEX off-gas (15-35 vol% CO and 20-35 vol% CO_2) to CO-richer converter off-gas (LDG; 60-70 vol% CO and 15-20 vol% CO_2), with blast-furnace gas and biomass- and coal-gasification gases occupying intermediate compositions (Fig. 2a). For COREX/FINEX, BFG and biomass-devided off-gases (CO/CO_2=1), this system yields 43.5 mmol/g DMC and 35.9 mL/g H_2, respectively (Fig. 2c). Increasing the CO/CO_2 molar ratio to 2 (coal-derived gas) a 67.8 mmol/g of DMC yield with 97.9% selectivity is obtained, and co-production of 65.2 mL/g of clean H_2 (Fig. 2c). As the CO fraction is increased across the tested CO/CO_2 molar ratio to 3 (LDG), the off-gas conversion system affords a DMC yield of 76.8 mmol/g with near 100% selectivity, nearly 7.8-fold higher than that obtained in the traditional CO_2 conversion system, together with the co-production of 74.6 mL/g of clean H_2 (Fig. 2b-c).

The effect of reaction temperatures on catalytic performance is shown in Fig. 2d. These trends are governed by the WGS reaction rate and DMC synthesis equilibrium. Specifically, the reaction temperature directly modulates byproduct H_2O accumulation, only of which determines the WGS reaction rate under high CO/H_2O molar ratio; the WGS rate then regulates the DMC synthesis equilibrium (Fig. S21). At low temperature of 120 °C, slow rate of MeOH and CO_2 limits H_2O and DMC generation and suppresses the downstream WGS reaction kinetics, resulting the decrease of DMC yield to 34.5 mmol/g with a 96.2% selectivity, and co-production H_2 of 31.1 mL/g (Fig. 2d). Raising the temperature to 140 °C, H_2O generation and conversion are kinetically matched, enabling a forward shift of the carbonate synthesis equilibrium, obtaining 68.5 mmol/g DMC with 97.9% selectivity, and 62.6 mL/g H_2 (Fig. 2d). Further increasing the temperature to 160 °C, the less favorable equilibrium of DMC synthesis reduces H_2O formation, thereby weakening the coupled WGS process and decreasing both DMC and H_2 yields to 38.8 mmol/g and 42.8 mL/g, respectively (Fig. 2d and Fig. S23). Overall, as intermediate in this new system, H_2O bridges WGS and DMC synthesis and enables their synergistic promotion. The regulation of reaction pressure also supports this view (Fig. S23).

To further reveal the H_2O-bridged coupling reaction path of off-gas and MeOH to DMC and H_2, isotope-labelling experiments are performed by partially replacing CH_3OH with CD_3OD (Fig. 2e-f). The liquid products show dominant molecular-ion signals at m/z = 90 and 93, which are assigned to $CH_3OCOOCH_3$ and $CD_3OCOOCH_3$, respectively, confirming that both CH_3OH and CD_3OD participate in DMC formation. H_2 and HD are simultaneously detected in the gas phase at m/z = 2 and 3, respectively. The formation of HD indicates that H_2O/HDO generated during DMC synthesis enters the LT-WGS reaction and contributes to H_2/HD formation, further indicating the bridging role of H_2O in the new off-gas conversion system.

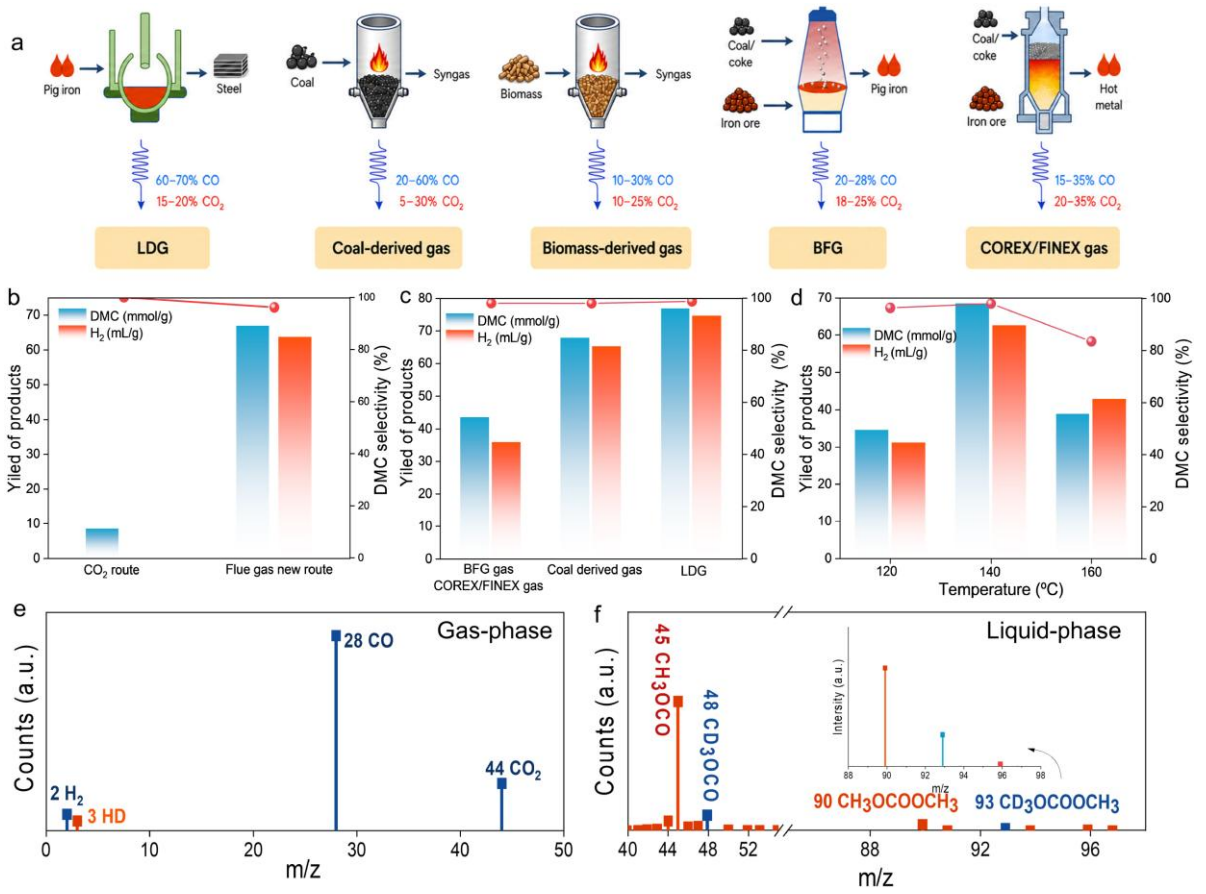


Fig. 2 Direct conversion of simulated industrial off-gas compositions. (a) Representative off-gas streams. (b) Comparison of DMC yield, H_2 yield, and DMC selectivity between the conventional CO_2 route and the new route. (c) DMC and H_2 yields and DMC selectivity for representative CO/CO_2 compositions. (d) Temperature dependence of DMC and H_2 yields and DMC selectivity. (e and f) Gas and liquid-phase mass spectra obtained in isotope-labelling experiments with partial replacement of CH_3OH by CD_3OD.

Reaction mechanisms of off-gas direct conversion to DMC and H_2

To reveal the reaction mechanism of the new route, we monitored surface intermediates by in-situ infrared spectroscopy. After MeOH adsorption, methoxy bands at ~1012, 1064 and 1116 cm^{-1} are observed both on CeO_2-600 and CeO_2-600/2%AuMoC-α, corresponding to terminal, bridged and multi-coordinated methoxy species(*22, 23*) (Fig. 3a-b and Fig. S24). Upon exposure to CO/CO_2, these methoxy species decrease while methyl carbonate intermediate (*CH_3OCOO) signals emerge at 1598, 1460, 1345 and 1197 cm^{-1} on both two catalysts, indicating coupling of activated *CO_2 and *CH_3O species to form *CH_3OCOO (*19, 22*) (Fig. 3a-b). Therefore, the off-gas and MeOH conversion process follows the reaction mechanism of *CH_3O+*CO_2→*CH_3OCOO+*CH_3O→DMC+H_2O, which is the same as CO_2-MeOH conversion mechanism. The difference is exhibited in gas DMC formation rate in LT-WGS driving. On flue-gas atmosphere, much higher IR signals of gas-phase DMC are observed at 1767 cm^{-1} and 1783 cm^{-1}, confirming enhanced DMC production in the coupling system(*24*) (Fig. 3c, Fig. S25). Overall, the off-gas does not change the DMC synthesis pathway, while significantly pulling the reaction equilibrium forward via in-situ H_2O conversion, thereby achieving efficient off-gas conversion and DMC synthesis.

Moreover, the diffusion and conversion of H_2O are verified by TPSR experiments. Under CO atmosphere, no CO_2 and H_2 signal is detected on CeO_2-600, consistent with its negligible WGS activity

(Fig. S26a). By contrast, H_2 and CO_2 are generated on 2%AuMoC-α at 100 °C, indicating low-temperature H_2O dissociation and reforming activity (Fig. S26b)(*18*), enabling high byproduct water conversion efficiency at low temperatures. To reveal H_2O diffusion from CeO_2-600 to 2%AuMoC-α and reaction with CO, the pre-hydrated CeO_2-600 is physically mixed with 2%AuMoC-α and gradually heats to 400 °C under CO atmosphere. In this process, clear CO_2 and H_2 signals are detected at 100 °C on the mixed catalyst, directly proving that H_2O can easily desorb from CeO_2-600, diffuse to 2%AuMoC-α, and react with CO to produce H_2 (Fig. S26c). This result confirms that the conversion of off-gas on this mixed catalyst follows a coupled reaction mechanism in which water migration and conversion act as linking steps (Fig. S26d).

To better understand the H_2O dissociation and its intermediate evolution, a key coupling reaction bridge of off-gas conversion route, we conducted quasi in-situ XPS experiments. 2%AuMoC-α catalyst shows characteristic C and Mo peaks from MoC-α (*25*) (Fig. S27). A peak at 530.7 eV is observed in the O 1s pattern, attributing to the residual oxygen (Or) on MoC-α(*26*). After H_2O exposure at room temperature, two new peaks emerge at ~532.0 and 532.4 eV, assigned to surface *OH species, alongside adsorbed H_2O at 535.2 eV, indicating H_2O dissociation into *OH on 2%AuMoC-α (*27, 28*) (Fig. S27). Correspondingly, the Mo-C peak in C 1s shifts to a lower binding energy of 283.2 eV, which can be related to electron transfer from *OH and *H to 2%AuMoC-α (Fig. S27, S29a) [25]. CO was then introduced into the system at 140 ºC for 30 min. The intensity of surface *OH species decreases significantly, indicating that *CO readily reacts with surface *OH species to produce CO_2 and H_2. Accompanied by *OH consumption, the C 1s peak shifts to 283.6 eV, which demonstrates that MoC-α is the primary site for the adsorption and dissociation of H_2O. The IR result could also support the reaction path of *CO and *OH (Fig. S28). However, a substantial amount of *OH species remain on MoC-α at 532.4 eV and is difficult to react further. This result indicates two types of *OH species on the MoC-α surface: those adjacent to Au and remote from Au sites. *OH species adjacent to Au can be eliminated by *CO adsorbed on Au, regenerating surface sites for further water dissociation, whereas *OH species far from Au remain as spectators(*28*) (Fig. S27).

When pre-hydrated CeO_2-600 was mixed with 2%AuMoC-α, the O 1s spectrum of the CeO_2-600/2%AuMoC-α shows not only residual oxygen and lattice oxygen from CeO_2-600 at 529.8 eV, but also *OH features at 532.7 and 531.9 eV(*27, 28*) (Fig. 3d). Consistently, the Mo–C component in the C 1s spectrum shifts to a lower binding energy of 283.9 eV (Fig. 3d and Fig. S29). These indicate that H_2O desorbed from CeO_2-600 can diffuse to 2%AuMoC-α and dissociate into *OH species. Subsequent exposure to CO at 140 °C led to a clear decrease in the intensity of surface *OH species, confirming the reforming of *OH species with CO(*26, 28*) (Fig. 3d). In the meantime, the C 1s peak shifts to 283.6 eV, reflecting the byproduct H_2O is absorbed and dissociated on MoC-α (Fig. 3d). Thus, the by-product H_2O can easily diffuse from CeO_2-600 to 2%AuMoC-α, as a bridge for the new route, dissociate into reactive *OH species on 2%AuMoC-α and yield H_2. In summary, the off-gas and MeOH co-conversion route does not change DMC formation pathway. The methoxy species couple with activated CO_2 to form

DMC and H_2O, and the generated H_2O diffuses to 2%AuMoC-α, undergoing dissociation into *OH and reacting with *CO to produce H_2. Continuous H_2O consumption through LT-WGS drives DMC synthesis equilibrium forward. Thus, H_2O serves as the bridge for CO_2 and CO simultaneous conversion, enabling the direct conversion of industrial off-gas and MeOH into DMC and H_2.

DFT calculations are performed to further understand the reaction pathway. For DMC synthesis on CeO_2, the weakened $*CH_3O$ adsorption facilitates coupling with activated CO_2 to form $*CH_3OCOO$ with a low barrier of 0.57 eV (Fig. 3e). The resulting $*CH_3OCOO$ intermediate dissociates one oxygen atom to form $*CH_3OCO$ intermediate. This step requires only barrier of 0.75 eV and becomes the rate-determining step for the overall DMC synthesis pathway (Fig. 3e). Finally, $*CH_3OCO$ couples with another methoxy species to produce DMC and H_2O (Fig. 3e). These results show that the synthesis of DMC on CeO_2-600 offers significantly kinetic advantages. The dissociated oxygen atom of $*CH_3OCOO$ is then readily hydrogenated in two consecutive steps to generate H_2O, with negligible barriers of 0.06 and 0.05 eV, respectively (Fig. 3e and Fig. S30).

After desorption, the full reaction pathway of H_2O conversion is analyzed. On the Au_{15}/ MoC-α model, water dissociates at the Au-MoC interfaces, whereas CO preferentially adsorbs on Au sites. H_2O dissociation proceeds with a barrier of 0.60 eV, and the resulting *OH reacts directly with *CO to form CO_2 and *H with a barrier of 0.72 eV, indicating a direct reforming pathway at the Au-MoC interfaces (Fig. 3f). By contrast, WGS on CeO_2 proceeds through the coupling of *CO and *OH to form *COOH, with an energy barrier of 0.88 eV (Fig. 3f). Although two surface H atoms are subsequently formed, their recombinative desorption as H_2 requires a much higher barrier of 3.12 eV (Fig. 3f). This high barrier accounts for the negligible LT-WGS activity of CeO_2 and shows that CeO_2 alone cannot promote DMC synthesis through in-situ H_2O conversion. Benefitting from the advantage of 2%AuMoC-α in H_2O conversion, the H_2 formation turnover frequency on Au_{15}/MoC-α is approximately 10 orders of magnitude higher than that on CeO_2 based on the transition state-theory-based microkinetic modelling (Fig. S31). Thus, H_2O conversion on 2%AuMoC-α bridges DMC synthesis and H_2 formation, thereby obtains a highly efficient direct off-gas utilization and MeOH upgrading.

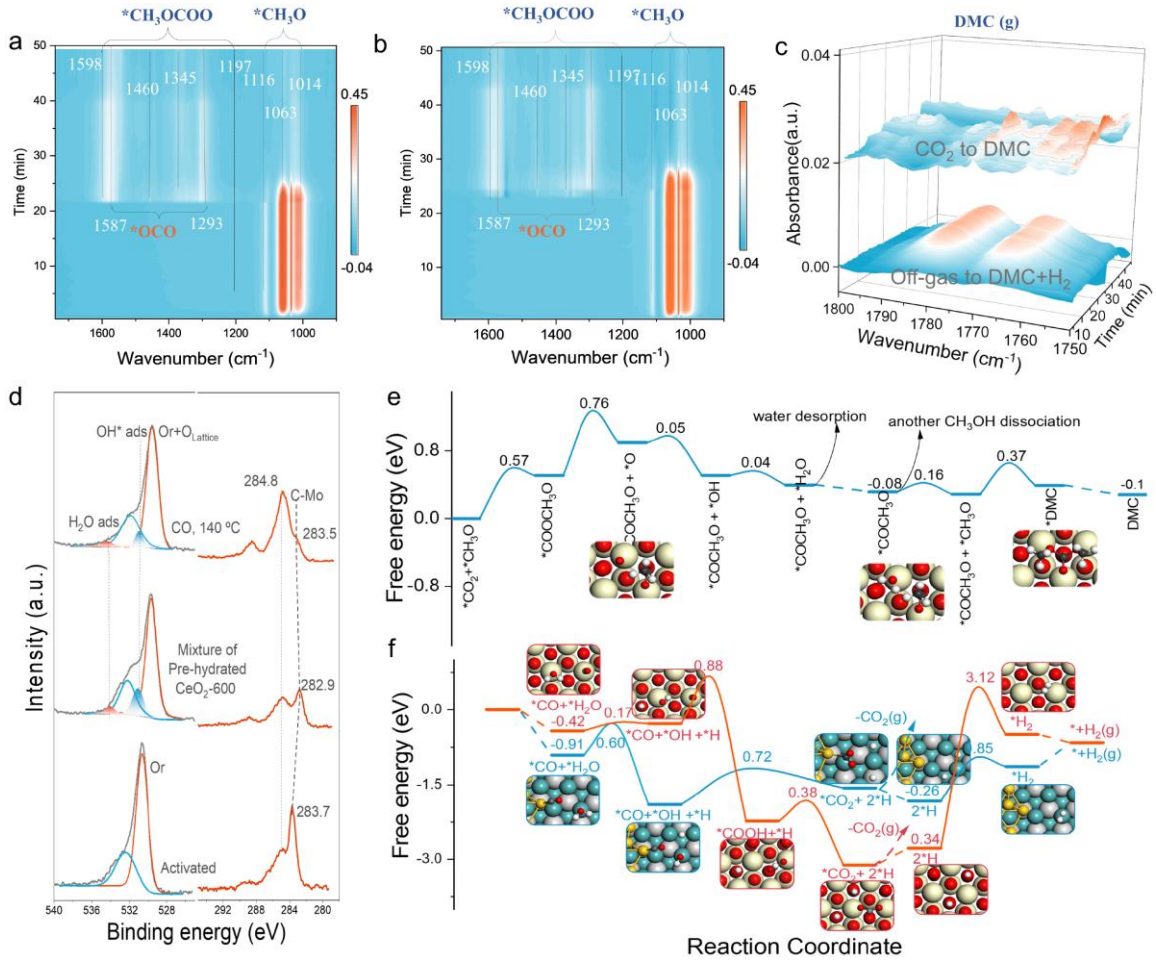


Fig. 3 Mechanistic of off-gas conversion to DMC and H_2. (a and b) Time-resolved in-situ infrared spectra of conventional CO_2 and off-gas routes, respectively. (c) Gas-phase DMC signals for the conventional CO_2 and off-gas routes. (d) Quasi in-situ XPS spectra following H_2O exposure and CO conversion on 2%AuMoC-α and the pre-hydrated mixed catalyst. (e) Calculated free-energy profile for DMC synthesis on CeO_2. (f) Calculated free-energy profiles for the LT-WGS reaction on Au_{15}/MoC-α and CeO_2.

Discussion

In this work, we demonstrate a direct conversion route of off-gas to DMC and H_2 via coupling industrial off-gas conversion and methanol upgrading. In the reaction system, CO_2 is fixed with MeOH to form DMC and by-product H_2O, while CO in-situ converts with H_2O into H_2 through LT-WGS, continuously driving the DMC formation equilibrium forward. A 76.8 mmol/g of DMC yield with near 100% selectivity is obtained on a physically mixed proof-of-concept CeO_2-600/2%AuMoC-α catalyst, 7.8 times higher than the conventional CO_2 route, together with 74.6 mL/g H_2 co-production. Mechanistic investigations show that methoxy species react with activated $*CO_2$ to form DMC and H_2O on CeO_2-600, the H_2O desorbs and diffuses to 2%AuMoC-α, where it dissociates into *OH at the Au-MoC interfaces and reacts with adsorbed CO to produce H_2. H_2O therefore functions as a bridge that connects CO_2 fixation with CO conversion. By simultaneously avoiding CO combustion, prior CO/CO_2 separation and external H_2 consumption, this work provides a resource-efficient route for industrial off-gas utilization and methanol upgrading. More broadly, it establishes a technical basis for developing carbon-efficient processes that directly convert complex industrial off-gas into value-added chemicals.

■ Methods

All experimental methods and details are provided in the Supplementary Information.

■ Associated Contents

Notes

The authors declare no competing financial interest.

■ Acknowledgement

This work was financially supported by the National Key Research and Development Plan Project of China (2022YFA1504700), Fundamental Research Funds for the Central Universities (2042026kf0011, 2042026fg0047), the National Natural Science Foundation of China (22273067, U22A20394, 22308266, U21A20317), Hubei Provincial Science and Technology Innovation Talent Program (2026DJA075), Natural Science Foundation of Wuhan (2026040301020033). The numerical calculations in this paper have been done on the supercomputing system in the Supercomputing Center of Wuhan University. We thank Dr. Lili Dai from the Core Facility of Wuhan University for his assistance with XPS analysis. We thank Professor Shizhou Pu from the School of Physics and Technology of Wuhan University for her assistance with STEM.

■ **Author Contributions** M.D designed the study. G.H performed most of the experiment. J.Z and X.G finished the DFT calculations. G.H, D.X and J.Z wrote the paper. The other author provided reagents and data analysis for the paper. G.H and J.Z have made an equal contribution to this work.

References

1. R. Bhimpuria, M. Tomar, A. Thapper, M. Ahlquist, K. E. Borbas, Photocatalytic product-selective reduction of CO_2, CO, and carbonates. *Chem* **11**, (2025).
2. P.-T. Wang, W.-T. Gao, F.-Y. Wang, M. Xu, X.-Y. Li, Carbon capture, utilization, and storage (CCUS) project optimization: multi-criteria deployment prioritization for China's coal chemical industry. *International Journal of Greenhouse Gas Control* **152**, (2026).
3. K. Kohse-Höinghaus, Combustion, Chemistry, and Carbon Neutrality. *Chemical Reviews* **123**, 5139–5219 (2023).
4. P. Wang *et al.*, Efficiency stagnation in global steel production urges joint supply- and demand-side mitigation efforts. *Nature Communications* **12**, 2066 (2021).
5. G. P. Thiel, A. K. Stark, To decarbonize industry, we must decarbonize heat. *Joule* **5**, 531–550 (2021).
6. J. Lee *et al.*, Molar-scale formate production via enzymatic hydration of industrial off-gases. *Nature Chemical Engineering* **1**, 354–364 (2024).
7. D. Wang, Z. Xie, M. D. Porosoff, J. G. Chen, Recent advances in carbon dioxide hydrogenation to produce olefins and aromatics. *Chem* **7**, 2277–2311 (2021).
8. L. Ding *et al.*, CO_2 Hydrogenation to Ethanol over Cu@Na-Beta. *Chem* **6**, 2673–2689 (2020).
9. J. Ye *et al.*, Hydrogenation of CO_2 for sustainable fuel and chemical production. *Science* **387**, eadn9388 (2025).
10. J. Zhu *et al.*, A New Class of Metal-Cyclam-Based Zirconium Metal–Organic Frameworks for CO_2 Adsorption and Chemical Fixation. *Journal of the American Chemical Society* **140**, 993–1003 (2018).
11. Y. F. Chen, M. Y. Qi, C. L. Tan, Z. R. Tang, Y. J. Xu, Methanol Upcycling Toward Glycolaldehyde Synthesis Enabled by New High‐Performance Photoredox Route. *Angewandte Chemie International Edition* **64**, (2025).
12. S. Chen *et al.*, Oxygen vacancy associated single-electron transfer for photofixation of CO2 to long-chain chemicals. *Nature Communications* **10**, 788 (2019).
13. D. Shi, S. Heyte, M. Capron, S. Paul, Catalytic processes for the direct synthesis of dimethyl

carbonate from CO_2 and methanol: a review. *Green Chemistry* **24**, 1067–1089 (2022).

14. W. Shao, X. Zhang, Y. Xie, Engineering active sites and recognizing mechanisms for CO2 fixation to dimethyl carbonate. *Trends in Chemistry* **5**, 312–323 (2023).

15. S. K. Kabra, E. Turpeinen, R. L. Keiski, G. D. Yadav, Direct synthesis of dimethyl carbonate from methanol and carbon dioxide: A thermodynamic and experimental study. *The Journal of Supercritical Fluids* **117**, 98–107 (2016).

16. Q. Cai, B. Lu, L. Guo, Y. Shan, Studies on synthesis of dimethyl carbonate from methanol and carbon dioxide. *Catalysis Communications* **10**, 605–609 (2009).

17. G. Hou *et al.*, Strongly Electron‐Accepting Lattice Oxygen of CeO_2 for Highly Efficient Dimethyl Carbonate Synthesis from CO_2 and Methanol. *Angewandte Chemie International Edition* **65**, (2025).

18. S. Yao *et al.*, Atomic-layered Au clusters on α-MoC as catalysts for the low-temperature water-gas shift reaction. *Science* **357**, 389–393 (2017).

19. G. Hou *et al.*, Dimethyl Carbonate Synthesis from CO_2 over CeO_2 with Electron-Enriched Lattice Oxygen Species. *Angewandte Chemie International Edition* **63**, e202402053 (2024).

20. M. Peng *et al.*, Thermal catalytic reforming for hydrogen production with zero CO_2 emission. *Science* **387**, 769–775 (2025).

21. R. Huang *et al.*, Acetylene hydrogenation to ethylene by water at low temperature on a Au/α-MoC catalyst. *Nature Catalysis* **6**, 1005–1015 (2023).

22. L. Li *et al.*, Atom‐Economical Synthesis of Dimethyl Carbonate from CO_2: Engineering Reactive Frustrated Lewis Pairs on Ceria with Vacancy Clusters. *Angewandte Chemie International Edition* **61**, (2022).

23. K. T. Jung, A. T. Bell, An in Situ Infrared Study of Dimethyl Carbonate Synthesis from Carbon Dioxide and Methanol over Zirconia. *Journal of Catalysis* **204**, 339–347 (2001).

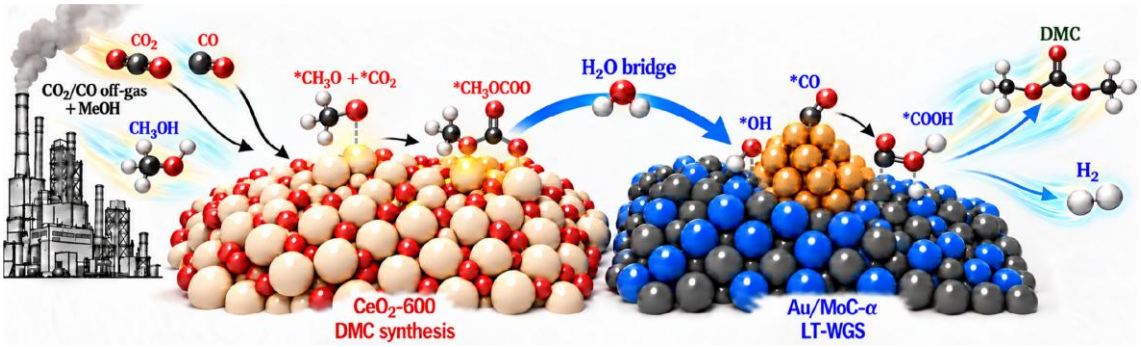
24. S. Chen *et al.*, Oxygen vacancy associated single-electron transfer for photofixation of CO(2) to long-chain chemicals. *Nat Commun* **10**, 788 (2019).

25. K. Murugappan *et al.*, Operando NAP-XPS unveils differences in MoO_3 and Mo_2C during hydrodeoxygenation. *Nature Catalysis* **1**, 960–967 (2018).

26. M. D. Porosoff, X. Yang, J. A. Boscoboinik, J. G. Chen, Molybdenum Carbide as Alternative Catalysts to Precious Metals for Highly Selective Reduction of CO_2 to CO. *Angewandte Chemie International Edition* **53**, 6705–6709 (2014).

27. K. Mudiyanselage *et al.*, Importance of the Metal–Oxide Interface in Catalysis: In Situ Studies of the Water–Gas Shift Reaction by Ambient-Pressure X-ray Photoelectron Spectroscopy. *Angewandte Chemie International Edition* **52**, 5101–5105 (2013).

28. X. Zhang *et al.*, A stable low-temperature H_2-production catalyst by crowding Pt on α-MoC. *Nature* **589**, 396–401 (2021).



A rationally designed coupled reaction network enables direct conversion of industrial off-gas (CO/CO_2) and methanol to green carbonate and H_2. In-situ produced byproduct H_2O bridge low-temperature WGS reaction to break the thermodynamic equilibrium constraint of DMC synthesis. The strategy converts the industrial off-gas utilization from a costly separation and high H_2 demand challenge into a reaction advantage for simultaneous DMC synthesis and H_2 production. Such coupling of off-gas utilization and methanol upgrading offers a feasible strategy for heavy industry decarbonization.

Supplementary Files

This is a list of supplementary files associated with this preprint. Click to download.

- SI.docx